Notch sensitivity of C/C-SiC composite evaluated by flexural tests☆

Yuan Shi [a,*,1], Yanlei Xiu [b,1], Peifang Wu [a], Can Wang [a], Yunjian Xiao [a], Raouf Jemmali [c], Daniel Cepli [c], Kamen Tushtev [d]

[a] Beijing Tianyishangjia New Material Corp., Ltd., Beijing, China
[b] Karlsruhe Institute of Technology, Karlsruhe, Germany
[c] Institute of Structures and Design, German Aerospace Center Stuttgart, Pfaffenwaldring 38-40, 70569 Stuttgart, Germany
[d] Advanced Ceramics, University of Bremen, Am Biologischen Garten 2, 28359 Bremen, Germany

Keywords:
Ceramic Matrix Composites
C/C-SiC
Flexural properties
Notch sensitivity
Work of fracture

A B S T R A C T

The notch effects on the mechanical behavior of Liquid Silicon Infiltration (LSI) based continuous carbon fiber reinforced silicon carbide (C/C-SiC) was studied. The in-plane (IP) and out-of-plane (OP) flexural properties of notched and unnotched samples with fiber orientations (0°, 45° and 60°) were determined through 3-point-bending (3PB) and single notched beam (SENB) tests. Despite the significant difference in bending modulus, the strength depends only slightly on the fiber orientation and loading direction, which could be explained through the uneven distribution of SiC-matrix within the block-like structure of C/C-SiC. This unique microstructure also leads to a relatively constant value of notch sensitivity in the IP direction, and the sensitivity to the notch is relatively low for all tested C/C-SiC specimen configurations. Furthermore, due to the large differences of fracture mechanism, the work of fracture (WOF) in the IP direction is significantly smaller than in the OP direction for all fiber orientations.

1. Introduction and objective

Ceramic matrix composites (CMCs) possess exceptional high-temperature capabilities, enhanced mechanical properties, and excellent corrosion resistance, making CMCs highly desirable for applications in the aerospace, energy, and automotive sectors [1–3]. The development of CMCs has focused on improving their processing techniques, enhancing the performance of reinforcing fibers, optimizing the matrix composition, and tailoring the interface between the matrix and fibers. Recently, the liquid silicon infiltration (LSI) process has emerged as a cost-effective method for producing continuous carbon fiber-reinforced silicon carbide (C/C-SiC) composites with desirable dense microstructures, oxidation resistance, and high-temperature strengths [4–6].

However, the presence of defects (e.g., holes, scratches, and cracks) can significantly affect the mechanical behavior of CMCs, influencing their fracture toughness and fatigue performance. The effects of notches and holes were studied intensively in the last decade of the 20th century [7–9]. It has been reported that reinforcement fibers could prevent crack propagation through the brittle ceramic matrix and enhance the crack resistance [10,11]. Experimental data showed that investigated CMCs are either insensitive or have limited sensitivity to the presence of notch [12,13]. The stress-redistribution and damage mechanisms around notches, such as multiple matrix cracking and shear bands damage, were extensively discussed, for example in [13–16].

In the past decades, numerous efforts have been dedicated to evaluate the fracture properties of notched CMCs in terms of tensile strength and flexural toughness [17,18]. For the tensile strength, an inelastic fracture mechanism with stress concentration/redistribution and the notch sensitivity factors have been investigated by various experimental and computational approaches [19–21]. Besides, three- and four-point bending tests are typical techniques to investigate the flexural characteristics of CMCs. In the work of Hofmann et al. [22] the ratio of bending to tensile strength and the work of fracture (WOF) of a LSI based C/C-SiC has been investigated through bending, tensile and single notched beam (SENB) tests, respectively, and the WOF was further used for a finite element analysis. The fracture behavior and fracture toughness of 2D

☆ In this study, all samples and experimental tests were manufactured and conducted at Institute of Structures and Design, German Aerospace Center Stuttgart (DLR)

* Corresponding author.
E-mail address: yuanshi@outlook.de (Y. Shi).

[1] These two authors contributed equally to this article

and 3D woven C/SiC composites, produced by LSI process, have been investigated using SENB specimens [23]. The study showed that the fracture toughness is mainly controlled by the nature of fracture, which is dictated by the differences in the fiber/matrix interface characteristics and by the weave conditions. SENB tests have been also used in the study of Yaghobizadeh et al. [24], focused on the evaluation of the effects of the phase composition on the mechanical properties of MAX phase-reinforced C/C-SiC composite, fabricated by LSI. The fracture properties of SiC/SiC composites have been investigated by Delage et al. [25] by means of tensile and flexural tests on notched specimens. Toughness mechanisms were identified and it was found that fracture toughness, expressed as stress intensity factor, is sensitive to displacement rate and fiber orientation (in-plane or out-of-plane).

Mao et al. [26] studied the fracture properties of C/SiC materials by SENB with a three-point bending (3PB) test, in which a full/local strain evolution and cracking growth during bending tests were thoroughly examined with the help of a digital image correlation (DIC) technique. Srivastava et al. [18] analyzed the critical stress intensity factors (SIFs) of the C/C-SiC composite under different loading conditions by split Hopkinson pressure bar (SHPB) and four-point bending tests. Nevertheless, the aforementioned flexural tests were mainly focused on the translaminar fracture, and very few of them placed emphasis on the interlaminar failure of CMCs.

Along with double-edge-notched tensile and SENB tests, some recent studies focus on single-edge-notched tensile tests (SENT) [27–29]. The standardized methods for evaluating fracture toughness do not consider the SENT specimen geometry, but it allows the use of digital image correlation (DIC) to study specimen failure originated from the notch.

To date, the fracture properties of CMC's have been studied mainly in the in-plane direction, using 0/90 specimens with notches perpendicular, respectively parallel to the fibers and loaded in the direction of the fiber reinforcement. Considering the multi-axial stress state occurring in many CMC-components, it is of great interest to understand the fracture mechanisms in out-of-plane direction and also as a function of fiber orientation.

In this work, a continuous carbon fiber reinforced C/C-SiC composite with carbon and silicon carbide matrix was fabricated by the liquid silicon infiltration (LSI) method. The fracture characteristics of these samples were investigated by three-point bending (3PB) tests associated with SENB methods. We further studied the notch sensitivity and fracture mechanisms in relation to loading directions as well as fiber orientations, which could be considered as extended research compared to the former work of Hofmann et al. [22] from same institute. The findings of this study will provide valuable insights into the notch effects on the mechanical behavior of C/C-SiC composites produced through LSI process. This knowledge will contribute to the continued development and advancement of CMCs, expanding their potential applications in various industries.

2. Experimental

2.1. Material C/C-SiC

In this work, a continuous carbon fiber reinforced C/C-SiC composite with carbon and silicon carbide matrix was tested, which was produced through Liquid Silicon Infiltration (LSI) technology at the Institute of Structures and Design of German Aerospace Center (DLR), Stuttgart, Germany.

In the first step, CFRP (Carbon Fiber Reinforced Polymers) preform was manufactured via warm pressing (T_{max}=240 °C, P_{max}=5.8 kPa) using prepregs based on a 2D carbon fiber fabric (woven plies of 3 K HTA fibers of Teijin Carbon Europe GmbH) and phenolic resin with approx. 60 mass % of carbon. To get a symmetrical structure, each single woven carbon fabric pre-infiltrated with phenolic resin was rotated by 90° during the ply stacking. Then, the CFRP plate was pyrolyzed at a temperature above 900 °C under an inert gas atmosphere, and the polymer matrix was transformed to a porous carbon matrix (C/C). During the pyrolysis process, the volatile components (such as ethanol, etc.) of the phenolic resin evaporate, and the matrix is converted in an amorphous and porous carbon matrix. Due to the mass loss of the matrix, this process is accompanied by approx. 10% shrinkage of the material in the thickness direction. Furthermore, due to the substantial shrinkage of the matrix, the carbon fibers are densely packed and embedded in the carbon matrix, a crack pattern (so-called "block structure" in Fig. 1b) evolves in a C/C body, which is essential for the silicon melt infiltration and prevents the reaction of the carbon fibers in C/C block with the liquid silicon. On the other hand, the block-wise structure provides local regions with agglomerations of silicon carbide (SiC) matrix without fiber reinforcement after siliconization (Fig. 1c), which could influence the failure path during mechanical tests. In the last step, liquid silicon was infiltrated into the porous C/C structure at T_{max} of approx. 1650 °C, which reacted with the carbon matrix to form SiC (Fig. 1c). The final C/C-SiC contains load-bearing carbon fiber bundles and a dense SiC matrix with a small amount of residual Si and C. The fiber volume content (FVC), porosity and density of the studied C/C-SiC plates are approx. 57.0%, 2.1% and 2.0 g/cm^3 , respectively. More details of the C/C-SiC manufacturing process can be found in previous publication [30].

2.2. Mechanical tests

The flexural properties of C/C-SiC samples with and without notches were determined and evaluated in different loading directions. All samples were cut from a C/C-SiC plate with fiber orientation 0/90° by using a diamond saw. The sample plan and the geometry of the different samples are shown in Fig. 2a and Fig. 2b, respectively. Samples without a notch submitted to flexural loading can be considered as standard 3-Point-Bending samples (3PB) and they were tested in In-Plane (IP) and Out-of-Plane (OP) directions with three different fiber orientations with regard to the longitudinal axis of the coupons: 0/90° (0°), ± 45° (45°) and + 60/ 30° (60°). The size of the 3PB sample (3PB-IP and 3PB-OP) is shown in Fig. 2b; the 3PB test was performed according to the DIN EN 658–3: 2002 [31]. Furthermore, Single-Edge Notched Bending (SENB) test according to the standard ASTM C1421–10b [32] has been used to obtain the notch sensitivity of C/C-SiC material, the notch having been prepared with a diamond saw with a width of 0.5 mm. It should be noted that ASTM C1421–10b is a standard for monolithic ceramics since no such standard exists for CMCs. Similar as 3PB, SENB coupons with 0°, 45° and 60° fiber orientations were also tested in IP and OP directions. The depth of the notch (a in Fig. 2b) was defined as half of the SENB sample thickness: 5 mm for the S-IP sample with a thickness of 10 mm; 3 mm for the S-OP sample with 6 mm thickness. In this way and due to the same specimen width, the cross-section of 3PB specimens is identical to the effective load-bearing area (the area above the notch) of SENB specimens in the same loading direction: 6 * 5 mm^2 (w*t) in IP direction and 4.8 * 3 mm^2 (w*t) in OP direction.

All the experiments were performed up to failure on a universal testing machine (Zwick 1494) at a controlled cross-head speed of 1 mm/min at room temperature. The measured force and displacement values are recorded simultaneously. For the 3PB tests, the longitudinal strains were measured with strain gauges on the tensile site of bending specimens. For statistical confirmation, four samples per series were tested.

3. Results of the mechanical tests

Typical force-displacement curves obtained in 3PB and SENB tests are shown in Fig. 3. It should be noted that the deflection of the bending specimens having not been measured directly, this is thus the cross-head displacement which is shown in the graphs. Furthermore, it should be pointed out that due to the different specimen geometry, both the maximum load and the slope of the curves for the in-plane and out-of-plane specimens are not directly comparable. Nevertheless, the force-displacement curves provide important details about the deformation

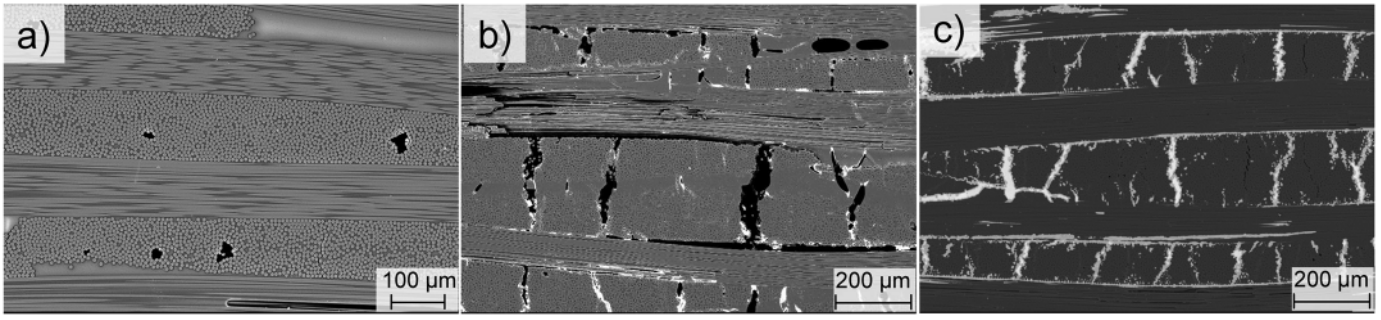

Fig. 1. Microstructure of C/C-SiC sample with 0/90° fiber orientation at different process steps: a) CFRP state, b) C/C state after pyrolysis with "block structure" and c) C/C-SiC after siliconization.
Reprinted with permission from ref. [30] Copyright © 2020 Elsevier Ltd.

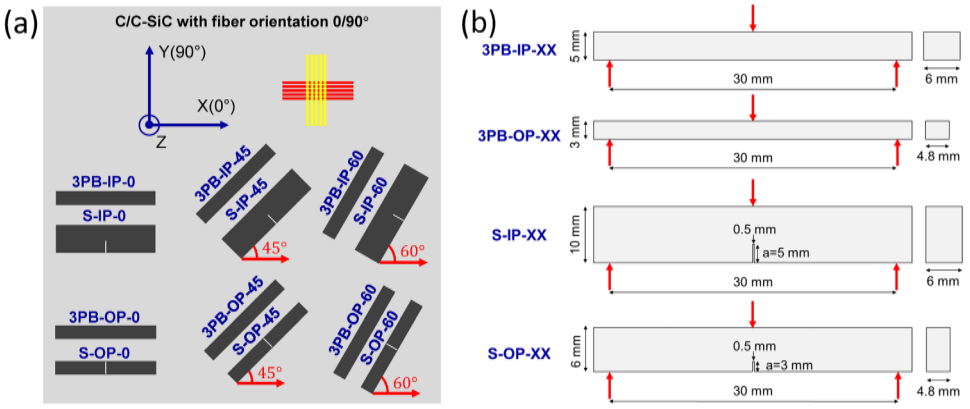

Fig. 2. (a) sample plan and (b) geometry of 3PB and SENB coupons with following acronyms: 3PB for 3-Point-Bending test, S for SENB test, IP for in-plane, OP for out-of-plan, 0° for 0/90°, 45° for ± 45° and 60° for + 60/− 30°.

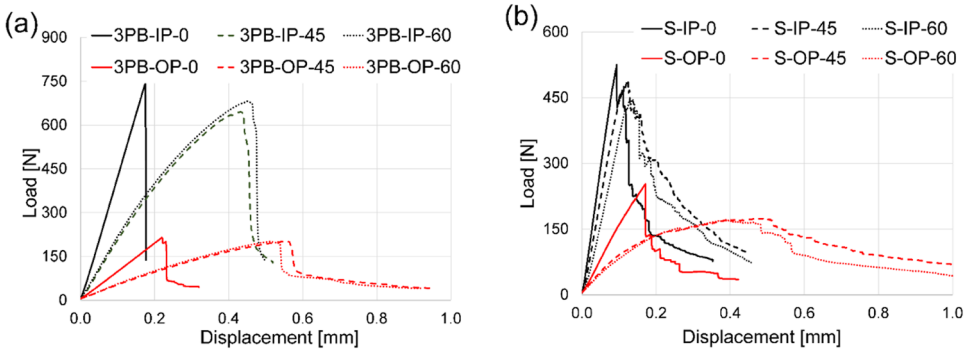

Fig. 3. Typical load-displacement-diagram of (a) 3PB and (b) SENB test with different fiber orientation in IP and OP directions.

processes as a function of the fiber orientation.

In both IP and OP directions, the 3PB specimens with 0° fiber orientation show nearly linear load-displacement behavior (Fig. 3a). In contrast, nonlinearities and therefore more significant deformation at maximum force are observed for samples with 45° and 60° fiber orientations. An almost sudden drop in force after reaching a maximum is besides observed in all samples.

A similar deformation behavior is also found for the SENB specimens (Fig. 3b). However, after the maximum force is reached, the notched specimens do not show a sudden drop but rather a continuous decrease in force and larger post-failure displacement. It should also be noted that the fiber orientation has a small effect on the material behavior in the IP direction, which can be seen from the minor difference between the load-displacement curves.

In addition to the force-displacement relationships, the strain on the tensile side of the 3PB specimens was recorded with strain gauges. It should be noted that because of the notch, no strain gauges were attached to the SENB specimens. Fig. 4 shows typical 3PB stress-strain curves of samples with fiber orientations at 0°, 45° and 60° in IP and OP directions. The C/C-SiC composite shows an almost linear behavior with high stiffness in both IP and OP directions, as seen in Fig. 4, when the tensile and compressive stresses acting under bending loading are aligned with one of the arrays of fiber tows (0° fiber orientation). In contrast, samples with 45° and 60° fiber orientation show clearly nonlinear behavior and considerably lower initial stiffness. Similar behavior of the investigated C/C-SiC has been observed under uniaxial tension and compression loadings [33]. It should be noted that the strain gauges usually failed as the maximum force was achieved during the

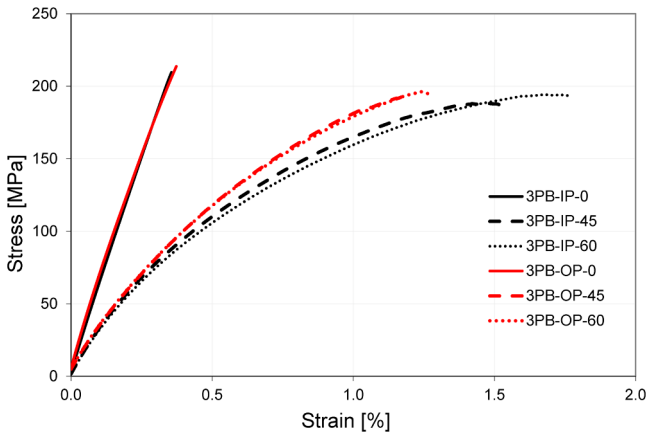

Fig. 4. Typical stress-strain-diagram of 3PB tests on samples with 0°, 45°, and 60° fiber orientation in IP and OP directions.

test. Therefore, no valuable data could be shown in the stress-strain curves in Fig. 4 beyond the failure of 3PB samples, compared to Fig. 3b.

The mean value and standard deviation of the flexural strength and bending modulus under 3PB loading for different fiber orientations in IP and OP directions are shown in polar plots (Fig. 5). Due to the symmetrical material configuration, it was assumed that the mechanical properties of 0° fiber orientation are equal to 90°, 180°, 270°, and 360°. The properties of 45° and 60° fiber orientations are plotted in Fig. 5 in the same manner as 135°, 225°, 315° and 30°, 120°, 150°, 210°, 240°, 300°, 330° respectively. The determination of the bending moduli was conducted using a linear fit of the initial linear region of the stress-strain curves displayed in Fig. 4 and the failure stress was calculated from the maximum load according to the associated standards. For the investigated three fiber orientations 0°, 45° and 60°, the 3PB flexural strength (Fig. 5a) and bending moduli (Fig. 5b) are almost equal in both IP and OP directions. Moreover, the flexural strength depends only slightly on the fiber orientation, so that an isotropy of the strength is almost present. In contrast, there is a strong anisotropy of the stiffness, with a bending modulus in the fiber direction (0°) being at least 2 times larger than in 45° and 60° fiber orientations.

It should be noted that, due to the limited size of the manufactured C/C-SiC plate, the bending properties with 0° fiber orientation in the OP direction were determined in this work by the 3PB test with a span-to-thickness (L/t) ratio of 10. In comparison, the flexural properties of identical composite were investigated previously with a L/t ratio of 20 [30] and both results are summarized in Table 1. According to this comparison (Table 1), the influence of different L/t ratios for C/C-SiC can be neglected.

Table 1
Comparison of the 3PB strength, bending modulus and fracture strain of identical C/C-SiC material with 0° fiber orientation under 3PB loading in OP direction through two different span-to thickness ratios (L/t).

	Strength [MPa]	Bending modulus [GPa]	Fracture strain [%]
C/C-SiC with L/t = 20[30]	209.1 ± 13.8	69.3 ± 2.2	0.41 ± 0.04
C/C-SiC with L/t = 10 [current]	209.8 ± 5.9	67.4 ± 3.5	0.36 ± 0.04

4. Discussion

4.1. Mechanical properties under 3PB loading

The C/C-SiC composite investigated here is characterized by carbon fiber bundles embedded in a SiC-matrix with a small amount of residual Si and C [30]. The block-like structure formed after the pyrolysis process and silicon infiltration [30] is essential for the material properties. As observed in previous studies [33], the C/C-SiC composite is characterized by load-sharing carbon fibers and behaves almost linearly in both pure tension and compression when the load is applied parallel to the fibers. As expected, the composite exhibits linear behavior under bending loads in the fiber orientation, both in-plane and out-of-plane (Fig. 4). In this case, due to the stiffer fibers and the highly inhomogeneous matrix, it can be assumed that the carbon fibers carry most of the load. For bending of samples with 45° and 60° orientations (Fig. 4), when the fibers are not directly loaded, the non-linearity of the stress-strain curves can also be explained by the matrix properties. Early microcrack formation and further crack growth in the inhomogeneous matrix could lead to a decrease in stiffness and a nonlinear stress-strain behavior. For bending in 45° and 60° orientations, high shear stresses also act parallel to the fibers, so the lower stiffness and the higher deformation of the composite are in good agreement with previous studies. In [33], it was found that the composite is relatively weak and deforms significantly at low stresses under shearing load applied in the fiber direction.

Despite the significant difference in bending modulus (Fig. 5b), all specimens fail at approximately the same stress, regardless of the fiber orientation (Fig. 5a), which could be explained through the block-like structure (Fig. 1b) that resulted from the manufacturing process. As presented in Section 2.1, the carbon fiber bundles are embedded within quasi-rectangular C/C blocks and the C/C structures are surrounded by SiC-matrix after siliconization (Fig. 1c). The porous pyrolytic C-matrix could be the key reason for the lower bending modulus for 45° and 60° fiber orientations. The similar strength of samples with different fiber orientations in IP direction may be explained by the distribution of the SiC-matrix, which fulfilled the crack pattern between the C/C blocks. According to the crack path of the tested 3PB samples, see Fig. 6a-c, the

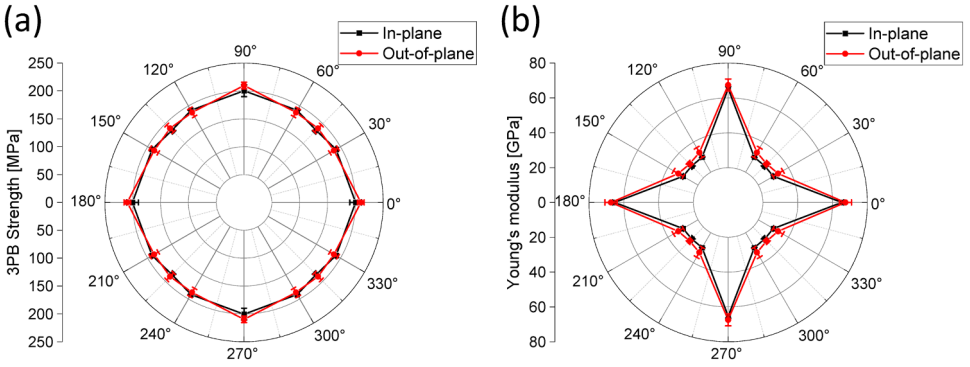

Fig. 5. Polar plot of (a) 3PB strength and (b) bending modulus of C/C-SiC with different fiber orientation in IP and OP direction.

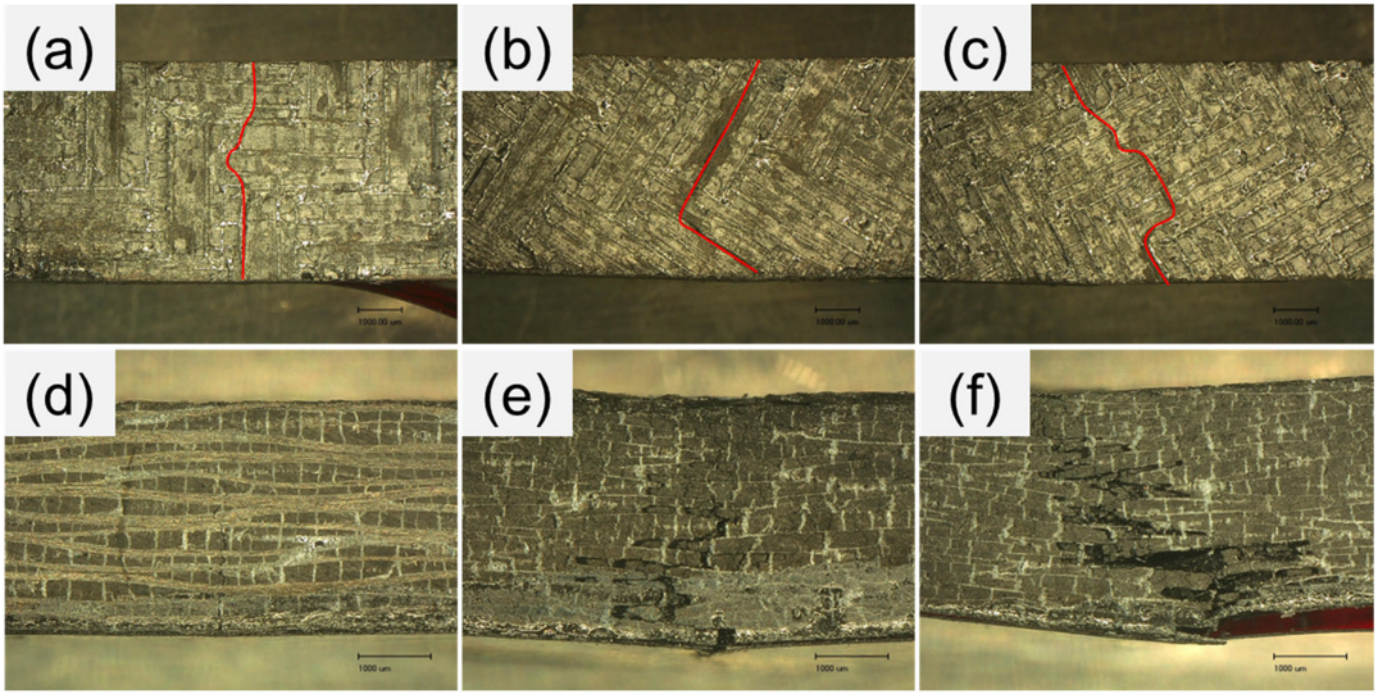

Fig. 6. Side view of crack path location of tested 3PB samples a) 3PB-IP-0; b) 3PB-IP-45; c) 3PB-IP-60; d) 3PB-OP-0; e) 3PB-OP-45; f) 3PB-OP-60.

failure always follows the fiber orientation and the cracks are almost straight with few deflections between the fiber bundles, which indicates that the crack path of C/C-SiC sample under bending load takes place in the SiC-rich region without fiber bundles. This kind of behavior is visible in all coupons, regardless of fiber orientations.

We have also hypothesized that in OP direction, the failure arises in the matrix-rich regions and the further crack propagation follows these areas. However, because the strength of the composite finally depends on the strength of the crack-bridging fiber bundles, the significantly longer crack path for 45° and 60° fiber orientations (see Fig. 6d-f) seems to affect only the dissipated mechanical energy and not the ultimate failure of the composite (see also section 4.3).

5. Notch sensitivity

Regarding the component's reliable design, the notch effects on the mechanical strength are of crucial interest. Defects on the surface of the material, such as scratches, cracks, etc., could reduce the strength of the material considerably and can cause it to be very different from that measured on specimens with a smooth surface. In this work, due to the identical effective bearing area of the 3PB and SENB samples, the notch sensitivity of the composite was evaluated by directly comparing the maximum force for unnotched and notched specimens. It should be noted that not only the effective bending thickness and the specimen width, but also the span of the 3PB and SENB specimens were identical. Thus, the maximum force of the SENB samples (with notch) was evaluated at different fiber orientations in IP and OP directions and subsequently normalized by the corresponding maximum force evaluated in the 3PB test (Fig. 7). According to the results displayed in Fig. 7, the notch sensitivity of the investigated C/C-SiC is relatively low for all tested specimen configurations. Similar to the 3PB results, the SENB strength in the IP direction is little influenced by the fiber orientation. Consequently, the notch sensitivity is rather constant, with mean values varying around 0.7. In contrast, the influence of the fiber orientation is much more pronounced in the OP direction. The notch sensitivity is in general lower and there was some indication of notch "strengthening" in 0° orientation.

When comparing the fracture of 3PB and SENB specimens, similar

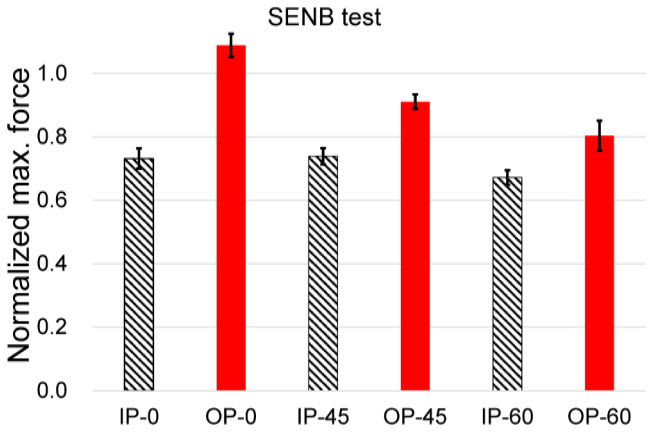

Fig. 7. Normalized maximum force of SENB tests at different fiber orientations in IP and OP directions.

failure patterns can be seen at the corresponding fiber orientations (Fig. 6 and Fig. 8). In the IP direction a main crack develops, which usually follows the fiber orientation. The comparable notch sensitivity of all IP samples could be explained by the unique block-wise microstructure of C/C-SiC, the failure paths are located in the SiC-rich area and between fiber bundle (Fig. 8a-c). In this way, the maximum force of SENB tests from IP direction is independent on the fiber orientation.

In contrast, the crack in the OP direction does not proceed in a straight line, but "jumps" between the neighboring layers. As can be seen in Fig. 8d, in the 0° samples in the OP direction, a main crack extends almost straight and perpendicular to the fibers oriented in the longitudinal direction of the sample. This indicates that the crack-bridging fibers determine the ultimate failure and the strength of the specimens, regardless of whether the main cracks originate from internal microcracks and defects in the matrix (3PB samples) or from artificially applied notches (SENB samples). This hypothesis may explain why the composite is evaluated as notch insensitive in 0° fiber orientation. In comparison, the main crack in the 45° and 60° OP-specimens propagates

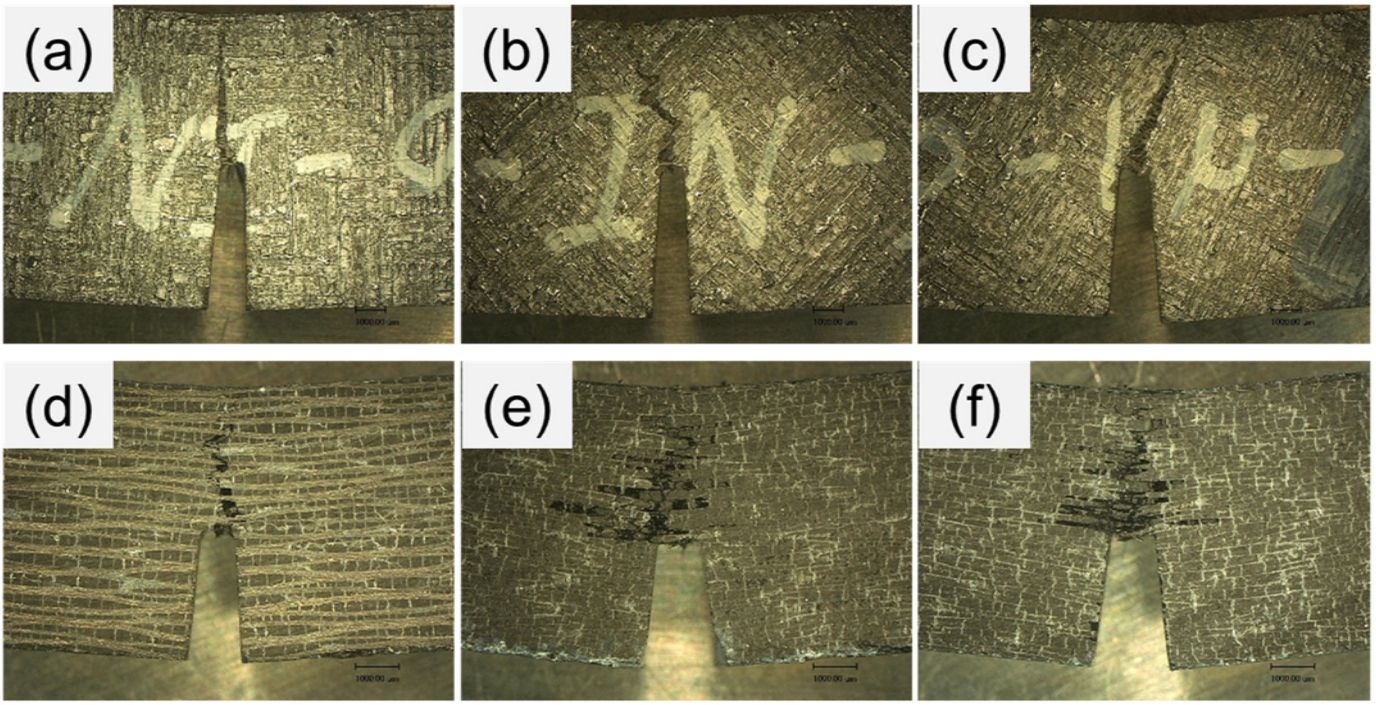

Fig. 8. Side view of crack path location of tested SENB samples a) S-IP-0; b) S-IP-45; c) S-IP-60; d) S-OP-0; e) S-OP-45; f) S-OP-60.

to a significantly higher extent in the matrix-rich region between the layers and thus follows the layer orientation (Fig. 8e and f). The crack extending into the specimen thickness is associated with failure of the overloaded fiber bundles, allowing the crack to propagate into the next matrix-rich regions. As already mentioned, the fracture spreads in this way over a large area of the specimen and, to a large extend, concerns the matrix, we have hypothesized that the applied notches in the SENB-specimens with 45° and 60° fiber orientation (S-OP-45 and S-OP-60), which cause local stress concentration, lead to earlier crack growth, and thus lower strength of the pre-notched specimens (SENB) compared to the unnotched ones (3PB). The slightly higher notch sensitivity of the specimens with 60° orientation can probably be explained by the more difficult fiber-bundle-pullout, due to the non-symmetrical fiber orientation relatively to the longitudinal axis of the specimen.

6. Fracture toughness and work of fracture

The fracture toughness in terms of the stress intensity factor K_{IC} was evaluated according to the standard ASTM C1421–10, using the results of the SENB tests. The calculated K_{IC} for the C/C-SiC composite at different orientation in IP and OP directions is shown in Fig. 9. For the IP direction, there is almost no dependence on the fiber orientation; the values obtained vary around 6 MPa $m^{½}$ or a slightly higher. A small dependence on the fiber orientation was found for the OP direction as the maximum and minimum values are 7.5 MPa $m^{½}$ at 0° orientation and 5.3 MPa $m^{½}$. at 45° orientation, respectively. It is worth mentioning that certain similarities can be seen in the notch sensitivity and the fracture toughness trends. As previously mentioned, the notch sensitivity in IP direction is rather independent on the fiber orientation, which also corresponds to a constant fracture toughness. Similarly, in the OP direction and 0° fiber orientation, the composite is notch insensitive, and consequently the fracture toughness reaches a higher value. It should be noticed that the K_{IC} measured in the former work of Hofmann et al. [22] are slightly lower, which can be explained by the fact that the manufacturing parameter of LSI based C/C-SiC has been optimized during the last decade at Institute of Structures and Design, German Aerospace Center Stuttgart [5,34].

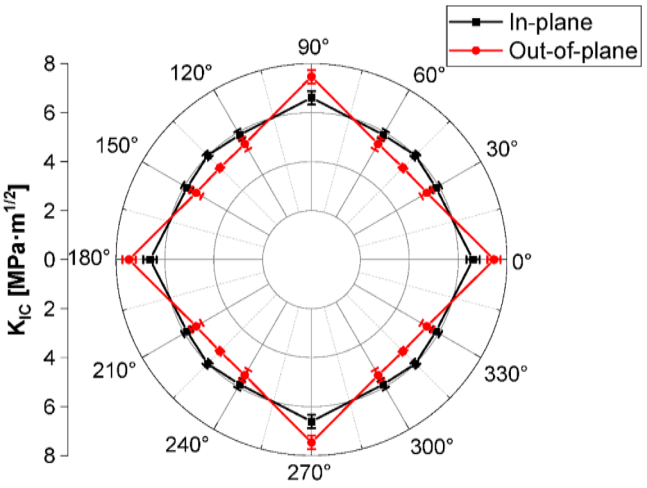

Fig. 9. Fracture toughness K_{IC} of C/C-SiC at different fiber orientations in IP and OP direction.

According to the ASTM C1421–10 the stress intensity factor K_{IC} was calculated using the maximum force and the initial notch length. In order to take the post failure behavior of the composites (Fig. 3) into account, the fracture energy release rate or work of fracture (WOF) was also evaluated in addition to the fracture toughness. The WOF was calculated for all the SENB specimens as the area under the load-deflection curves (which corresponds to the fracture energy). Fig. 10 shows the WOF calculated up to maximum force Fmax (Fig. 10 a) and after fracture up to a force decrease of 30% Fmax (Fig. 10 b) and illustrates the dependence of the WOF on the fiber orientation for IP and OP directions.

Since the deflection of the SENB specimens was not measured directly, the compliance of the testing machine and bending device was determined by comparing the cross-head displacement to the measured strain on the tensile side of the 3PB specimens. The compliance determined in this way was used for correcting the cross-head displacement of

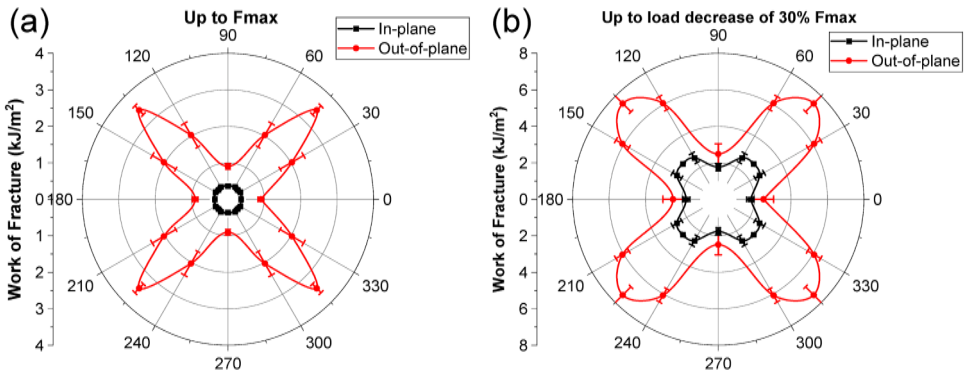

Fig. 10. Work of fracture of SENB tests: (a) up to Fmax and (b) up to decrease of 30% Fmax.

the SENB specimens and determining their actual deflection.

First of all, it should be mentioned that the WOF for IP direction is significantly smaller than in OP direction for all fiber orientations. A possible explanation for the large differences in WOF could be found when analyzing the fracture surfaces of the SENB samples. As can be seen in Fig. 8, the fracture surfaces reveal significant differences in the failure mode of the SENB specimens in IP and OP direction. In the IP direction, there is usually a main crack that extends parallel to the fibers. Consequently, the crack goes almost straight to the edge of the specimen and is relatively short. However, the samples with 45° and 60° orientation have a slightly longer failure path and therefore dissipate a slightly higher energy compared to the samples with 0° orientation. This difference is more obvious when the fracture energy is evaluated up to 30% of Fmax (Fig. 10 b). In general, completely different failure is observed in the OP direction Fig. 8d-f). The crack is strongly deflected between the layers, which also leads to the fiber bundle pull-out. With the 45° and 60° fiber orientations, the fracture zone especially includes a large area in front of the notch tip, which leads to considerably higher energy dissipation. Consequently, a significantly higher WOF was calculated.

7. Conclusions

In this work, the effect of the notch on the mechanical behavior of LSI based C/C-SiC composite was investigated. The flexural behavior of notched and unnotched specimens was analyzed and compared in terms of maximum load, fracture toughness, and work of fracture. Particular attention was paid to understanding in-plane and out-of-plane fracture mechanisms as a function of fiber orientation (on-axis and off-axis). The calculated K_{IC}, WOF up to Fmax and up to decrease of 30% Fmax for different fiber orientation and loading direction are summarized in Table 2. The main conclusions of this work are:

- The flexural properties of C/C-SiC with three different fiber orientations (0°, 45°, and 60°) were determined in IP and OP directions through the 3PB test. Although the bending moduli are almost the same in both IP and OP directions, the value in the fiber direction 0° is approx. 2 times higher than in 45° and 60° directions. However, an isotropy of the flexural strength can be observed regardless of orientation and loading direction, which could be explained through the distribution of SiC-matrix within the unique block-like structure of C/C-SiC: the failure cracks are near the SiC-rich region and always follow the fiber bundle orientation with few deflections.
- The notch sensitivity of C/C-SiC was evaluated by directly comparing the maximum forces for unnotched (3PB) and notched (SENB) specimens. The composite is notch insensitive for all tested specimen configurations: the mean value varies around 0.7 in the IP direction for all three fiber orientations; a more pronounced influence of orientation can be observed in the OP direction, and the minimum value is approx. 0.8 at 60°. This different notch sensitivity could also be explained through failure patterns resulting from the block-wise structure. Since the failure paths follow the fiber orientation and locate in the SiC-rich area, the maximum force of SENB tests in the IP direction is independent on the fiber orientation. In contrast, the crack in the OP direction propagates between the neighboring layers and thus follows the layer orientation, in which the fracture spreads over a large area of the specimen and concerns to a large extent the matrix.
- The fracture toughness in terms of stress intensity factor shows a slight dependence on the fiber orientation and loading direction and varies between 5.3 MPa m½ and 7.5 MPa m½. The WOF was calculated for all the SENB specimens as the area under the load-deflection curves (corresponding to the fracture energy). The value of WOF and the dependence of orientation for OP are significantly higher than in the IP direction. In the IP direction, the crack goes almost straight to the edge of the specimen and is relatively short. However, a completely different failure is observed in the OP direction and the crack is strongly deflected between the layers. This also leads to the fiber bundle pull-out, especially in the 45° fiber orientation, which leads to considerably higher energy dissipation.

The results in this work show that C/C-SiC material has excellent notch insensitivity properties. The flexural strength is almost isotropic and the WOF of 45° fiber orientation in the OP direction is relatively high. These results may help to design and develop C/C-SiC structures to meet stiffness, strength, notch sensitivity, fracture toughness, and fracture energy requirements.

Table 2
Summary of calculated K_{IC}, WOF up to Fmax and up to decrease of 30% Fmax for different fiber orientation and loading direction.

Fiber orientation	Loading direction	K_{IC} [MPa m½]	WOF up to Fmax [kJ/m²]	WOF up to decrease of 30% Fmax [kJ/m²]
0/90° (0°)	In-plane	6.61 ± 0.27	0.36 ± 0.05	1.76 ± 0.20
	Out-of-plane	7.46 ± 0.27	0.90 ± 0.08	2.49 ± 0.56
±45° (45°)	In-plane	6.01 ± 0.15	0.37 ± 0.06	2.75 ± 0.05
	Out-of-plane	5.29 ± 0.11	3.45 ± 0.17	7.42 ± 0.63
+ 60/ 30° (60°)	In-plane	5.87 ± 0.21	0.39 ± 0.03	2.62 ± 0.29
	Out-of-plane	5.45 ± 0.27	2.03 ± 0.37	6.08 ± 0.41

CRediT authorship contribution statement

Yuan Shi: Conceptualization, Data curation, Methodology, Visualization, Writing – priginal draft preparation. **Yanlei Xiu**: Visualization, Writing – original draft preparation. **Peifang Wu**: Resources. **Can Wang**: Validation. **Yunjian Xiao**: Validation. **Raouf Jemmali**: Data curation, Investigation. **Daniel Cepli**: Data curation, Investigation. **Kamen Tushtev**: Conceptualization, Data curation, Writing – review & editing.

Declaration of Competing Interest

The authors declare that they have no known competing financial interests or personal relationships that could have appeared to influence the work reported in this paper.

Acknowledgment

We want to thank Yikun Li at the Beijing Tianyishangjia New Material Corp., Ltd. for the collaboration and support for this work. This research did not receive any specific grant from funding agencies in the public, commercial, or not-for-profit sectors.

References

[1] N.P. Bansal, J. Lamon, Ceramic Matrix Composites: Materials, Modeling and Technology, John Wiley & Sons, 2014.
[2] A.G. Evans, D.B. Marshall, Overview no. 85 The mechanical behavior of ceramic matrix composites, Acta Metall. 37 (10) (1989) 2567–2583.
[3] F.W. Zok, C.G. Levi, Mechanical properties of porous-matrix ceramic composites, Adv. Eng. Mater. 3 (1–2) (2001) 15–23.
[4] W. Krenkel, F. Berndt, C/C–SiC composites for space applications and advanced friction systems, Mater. Sci. Eng.: A 412(1-2) (2005) 177–181.
[5] B. Heidenreich, Manufacture and Applications of C/C-SiC and C/SiC Composites, Processing and Properties of Advanced Ceramics and Composites IV2012, pp. 183–198.
[6] M. Patel, K. Saurabh, V.V.B. Prasad, J. Subrahmanyam, High temperature C/C–SiC composite by liquid silicon infiltration: a literature review, Bull. Mater. Sci. 35 (1) (2012) 63–73.
[7] W.P. Keith, K.T. Kedward, Notched strength of ceramic-matrix composites, Compos. Sci. Technol. 57 (6) (1997) 631–635.
[8] Y. Kogo, H. Hatta, H. Kawada, T. Machida, Effect of stress concentration on tensile fracture behavior of carbon-carbon composites, J. Compos. Mater. 32 (13) (1998) 1273–1294.
[9] V.A. Kramb, R. John, L.P. Zawada, Notched fracture behavior of an oxide/oxide ceramic-matrix composite, J. Am. Ceram. Soc. 82 (11) (1999) 3087–3096.
[10] Y.-H. Cha, K.-S. Kim, D.-J. Kim, Evaluation on the fracture toughness and strength of fiber reinforced brittle matrix composites, KSME Int. J. 12 (3) (1998) 370–379.
[11] Z. Suo, S. Ho, X. Gong, Notch ductile-to-brittle transition due to localized inelastic band, J. Eng. Mater. Technol. -Trans. Asme 115 (3) (1993) 319–326.
[12] J.C. McNulty, F.W. Zok, G.M. Genin, A.G. Evans, Notch-sensitivity of fiber-reinforced ceramic-matrix composites: effects of inelastic straining and volume-dependent strength, J. Am. Ceram. Soc. 82 (5) (1999) 1217–1228.
[13] T.J. Mackin, T.E. Purcell, M.Y. He, A.G. Evans, Notch sensitivity and stress redistribution in three ceramic-matrix composites, J. Am. Ceram. Soc. 78 (7) (1995) 1719–1728.
[14] M.Y. He, B. Wu, Z. Suo, Notch-sensitivity and shear nands in brittle-matrix composites, Acta Metall. Et. Mater. 42 (9) (1994) 3065–3070.
[15] F.E. Heredia, S.M. Spearing, T.J. Mackin, M.Y. He, A.G. Evans, P. Mosher, P. Brøndsted, Notch effects in carbon matrix composites, J. Am. Ceram. Soc. 77 (11) (1994) 2817–2827.
[16] C.M. Cady, T.J. Mackin, A.G. Evans, Silicon carbide/calcium aluminosilicate: a notch-isensitive ceramic-matrix composite, J. Am. Ceram. Soc. 78 (1) (1995) 77–82.
[17] M.A. Mattoni, F.W. Zok, Strength and Notch Sensitivity of Porous-Matrix Oxide Composites, J. Am. Ceram. Soc. 88 (6) (2005) 1504–1513.
[18] V.K. Srivastava, K. Maile, Measurement of critical stress intensity factor in C/C–SiC composites under dynamic and static loading conditions, Compos. Sci. Technol. 64 (9) (2004) 1209–1217.
[19] A. Haque, L. Ahmed, A. Ramasetty, Stress concentrations and notch sensitivity in woven ceramic matrix composites containing a circular hole-an experimental, analytical, and finite element sudy, J. Am. Ceram. Soc. 88 (8) (2005) 2195–2201.
[20] J.S. Park, Y. Katoh, A. Kohyama, S.P. Lee, H.K. Yoon, Evaluation of fracture toughness of ceramic matrix composites using small specimens, Fusion Eng. Des. 61-62 (2002) 733–738.
[21] M.B. Ruggles-Wrenn, G. Kurtz, Notch sensitivity of fatigue behavior of a Hi-Nicalon™/SiC-B4C composite at 1,200 °C in air and in steam, Appl. Compos. Mater. 20 (5) (2013) 891–905.
[22] S. Hofmann, B. Öztürk, D. Koch, H. Voggenreiter, Experimental and numerical evaluation of bending and tensile behaviour of carbon-fibre reinforced SiC, Comp. Part A 43 (11) (2012) 1877–1885.
[23] A.G. Paradkar, N. Shanti Ravali, N. Eswara Prasad, Mechanical behavior of 2D and 3D weaved SiC-matrix, carbon-continuous-fibre-reinforced composites: Part 2. Fracture toughness under static loading conditions, Eng. Fract. Mech. 182 (2017) 52–61.
[24] O. Yaghobizadeh, A. Sedghi, H.R. Baharvandi, Mechanical properties and microstructure of the C-C-SiC, C-C-SiC-Ti3SiC2 and C-C-SiC-Ti3Si(Al)C2 composites, Mater. Sci. Eng. A 731 (2018) 446–453.
[25] J. Delage, E. Saiz, N. Al Nasiri, Fracture behaviour of SiC/SiC ceramic matrix composite at room temperature, J. Eur. Ceram. Soc. 42 (7) (2022) 3156–3167.
[26] W.G. Mao, J. Chen, M.S. Si, R.F. Zhang, Z.B. Peng, C.Y. Dai, Q.S. Ma, D.N. Fang, Study of mechanical properties and cracking extension resistance behavior of C/SiC composites by single edge notched beam and digital image correlation techniques, Mater. Sci. Eng.: A 649 (2016) 222–228.
[27] P. Meyer, A.M. Waas, Experimental results on the elevated temperature tensile response of SiC/SiC ceramic matrix notched composites, Composites Part B: Engineering 143 (2018) 269–281.
[28] K. Ramachandran, S. Leelavinodhan, C. Antao, A. Copti, C. Mauricio, Y.L. Jyothi, D.D. Jayaseelan, Analysis of failure mechanisms of Oxide - Oxide ceramic matrix composites, J. Eur. Ceram. Soc. 42 (4) (2022) 1626–1634.
[29] D. Zhang, P. Meyer, A.M. Waas, An experimentally validated computational model for progressive damage analysis of notched oxide/oxide woven ceramic matrix composites, Compos. Struct. 161 (2017) 264–274.
[30] Y. Shi, F. Kessel, M. Friess, N. Jain, K. Tushtev, Characterization and modeling of tensile properties of continuous fiber reinforced C/C-SiC composite at high temperatures, J. Eur. Ceram. Soc. 41 (5) (2021) 3061–3071.
[31] D.D.I.f.N. e.V., Mechanical properties of ceramic composites at room temperature – Part 3: Determination of flexural strength, Beuth Verlag GmbH, Berlin, 2002.
[32] A.C.o.C.o.A. Ceramics, Standard test methods for determination of fracture toughness of advanced ceramics at ambient temperature, ASTM International,, 2010.
[33] Y. Shi, S. Li, E. Sitnikova, D. Cepli, D. Koch, Experimental evaluation and theoretical prediction of elastic properties and failure of C/C-SiC composite, Int. J. Appl. Ceram. Technol. 19 (1) (2021) 7–21.
[34] F. Breede, D. Koch, E. Maillet, G.N. Morscher, Modal acoustic emission of damage accumulation in C/C–SiC composites with different fiber architectures, Ceram. Int. 41 (9, Part B) (2015) 12087–12098.